

RESEARCH PAPER

The disruption of invariant natural killer T cells exacerbates cardiac hypertrophy and failure caused by pressure overload in mice

Masashige Takahashi¹ | Shintaro Kinugawa¹  | Shingo Takada¹  |
 Naoya Kakutani¹ | Takaaki Furihata¹ | Mochamad Ali Sobirin² | Arata Fukushima¹ |
 Yoshikuni Obata¹ | Akimichi Saito¹ | Naoki Ishimori¹ | Kazuya Iwabuchi³ |
 Hiroyuki Tsutsui⁴

¹Department of Cardiovascular Medicine, Faculty of Medicine and Graduate School of Medicine, Hokkaido University, Sapporo, Japan

²Faculty of Medicine, Diponegoro University, Semarang, Indonesia

³Department of Immunobiology, Kitasato University School of Medicine, Kanagawa, Japan

⁴Department of Cardiovascular Medicine, Faculty of Medical Sciences, Kyushu University, Fukuoka, Japan

Correspondence

Shintaro Kinugawa, Department of Cardiovascular Medicine, Faculty of Medicine and Graduate School of Medicine, Hokkaido University, Kita-15, Nishi-7, Kita-ku, Sapporo 060-8638, Japan.
 Email: tuckahoe@med.hokudai.ac.jp

Edited by: Andy Trafford

Funding information: This work was supported in part by grants from Japanese Grant-In-Aid for Scientific Research: JP26350879 (to S.K.), JP26750331 (to S.T.), JP16K16607 (to H.T.), JP17K15979 (to T.F.), JP17K10137 (to A.F.) and JP17H04758 (to S.T.).

Abstract

Chronic inflammation is involved in the development of cardiac remodelling and heart failure (HF). Invariant natural killer T (iNKT) cells, a subset of T lymphocytes, have been shown to produce various cytokines and orchestrate tissue inflammation. The pathophysiological role of iNKT cells in HF caused by pressure overload has not been studied. In the present study, we investigated whether the disruption of iNKT cells affected this process in mice. Transverse aortic constriction (TAC) and a sham operation were performed in male C57BL/6J wild-type (WT) and iNKT cell-deficient *Jα18* knockout (KO) mice. The infiltration of iNKT cells was increased after TAC. The disruption of iNKT cells exacerbated left ventricular (LV) remodelling and hastened the transition to HF after TAC. Histological examinations also revealed that the disruption of iNKT cells induced greater myocyte hypertrophy and a greater increase in interstitial fibrosis after TAC. The expressions of interleukin-10 and tumour necrosis factor- α mRNA and their ratio in the LV after TAC were decreased in the KO compared with WT mice, which might indicate that the disruption of iNKT cells leads to an imbalance between T-helper type 1 and type 2 cytokines. The phosphorylation of extracellular signal-regulated kinase was significantly increased in the KO mice. The disruption of iNKT cells exacerbated the development of cardiac remodelling and HF after TAC. The activation of iNKT cells might play a protective role against HF caused by pressure overload. Targeting the activation of iNKT cells might thus be a promising candidate as a new therapeutic strategy for HF.

KEYWORDS

cardiac failure, cardiac hypertrophy, hypertrophy, inflammation, natural killer T cells

1 | INTRODUCTION

Left ventricular (LV) hypertrophy in response to pressure overload is initially an adaptive process that normalizes wall stress and preserves contractile performance. However, sustained mechanical stress can result in the progression to maladaptive hypertrophy and cause the development of cardiac remodelling and heart failure (HF). Various molecular mechanisms underlying maladaptive hypertrophy

and HF in response to mechanical stress are known, and several pro-inflammatory cytokines, including interleukin (IL)-6 and tumour necrosis factor- α (TNF- α), have important roles in these mechanisms (Fischer & Hilfiker-Kleiner, 2007; Sun et al., 2007).

It has been reported that pressure overload and ischaemia induce cardiac inflammation in association with the upregulation of chemokines and the infiltration of inflammatory cells, and these have important roles in the development of cardiac fibrosis (Nicoletti &

Michel, 1999; Xia et al., 2009). In contrast, chronic inflammation was also reported to have protective effects during the maladaptive transition from hypertrophy to HF (Higuchi et al., 2004; Hirota et al., 1999). These findings suggested that: (i) cardiac inflammation might have bidirectional roles in the pathophysiology of HF; and (ii) the immunological modulation of a comprehensive cytokine network rather than the regulation of a single cytokine might be a suitable treatment strategy for patients with HF.

Invariant natural killer T (iNKT) cells are an innate-like T lymphocyte population that recognizes glycolipid ligands in the context of the protein CD1d. These cells are characterized by the coexpression of natural killer (NK) markers and the lipid-specific T-cell receptor (TCR) combined with a canonical $V\alpha 14$ - $J\alpha 18$ chain with the variable $V\beta 8$, $V\beta 7$ or $V\beta 2$ in mice or $V\beta 8$ or $V\beta 11$ in humans (Godfrey, MacDonald, Kronenberg, Smyth, & Van Kaer, 2004; Kronenberg & Gapin, 2002). The synthetic glycolipid α -galactosylceramide (α GC) specifically activates CD1d-restricted iNKT cells (Kawano et al., 1997). Upon activation, the iNKT cells have the capacity to secrete rapidly a mixture of large amounts of T-helper type 1 (Th1) and type 2 (Th2) cytokines plus a vast array of chemokines that shape the subsequent adaptive immune response (Matsuda, Malleveay, Scott-Browne, & Gapin, 2008). Thus, iNKT cells can function as a bridge between the innate and adaptive immune systems, and very few iNKT cells adequately conduct various immune cells and orchestrate tissue inflammation.

Indeed, iNKT cells are known to play a protective role in autoimmune and inflammatory diseases, such as type 1 diabetes, experimental allergic encephalomyelitis and rheumatoid arthritis (Hong et al., 2001; Miellot et al., 2005; Sharif et al., 2001; Singh et al., 2001). We reported that the activation of iNKT cells by α GC ameliorated cardiac remodelling and HF after myocardial infarction (MI) in mice (Sobirin et al., 2012). However, to date, no studies have examined the pathophysiological roles of iNKT cells in the development of cardiac hypertrophy and HF.

In the present study, we evaluated the effects of a targeted deletion of the iNKT gene on mortality and LV structural and functional alterations during pressure-overloaded cardiac hypertrophy. We used $J\alpha 18^{-/-}$ (formerly called $J\alpha 28^{-/-}$) mice with targeted disruption of the $J\alpha 18$ gene, resulting in the selective depletion of CD1d-dependent $V\alpha 14$ iNKT cells (Cui et al., 1997; Rogers et al., 2008).

2 | METHODS

2.1 | Ethical approval

All procedures and animal care in this study (approval no. 16-0101) were approved by Hokkaido University Graduate School of Medicine Committee on Animal Resources and conformed to the guiding principles in the care and use of animals of the American Physiological Society and the *Guide for the Care and Use of Laboratory Animals* of the National Research Council. At the end of the experiment, the mice were anaesthetized with an intraperitoneal (I.P.) injection of an overdose of pentobarbitone sodium (100 mg kg⁻¹, Somnopenty; Kyoritsu

New Findings

- **What is the central question of this study?**

We questioned whether the disruption of invariant natural killer T (iNKT) cells exacerbates left ventricular (LV) remodelling and heart failure after transverse aortic constriction in mice.

- **What are the main findings and their importance?**

Pressure overload induced by transverse aortic constriction increased the infiltration of iNKT cells in mouse hearts. The disruption of iNKT cells exacerbated LV remodelling and hastened the transition from hypertrophy to heart failure, in association with the activation of mitogen-activated protein kinase signalling. Activation of iNKT cells modulated the immunological balance in this process and played a protective role against LV remodelling and failure.

Seiyaku, Tokyo, Japan) and killed by collection of blood from the abdominal aorta.

2.2 | Animals and experimental protocol

$V\alpha 14^{+}$ NKT cell-deficient $J\alpha 18^{-/-}$ (KO) mice were provided by Dr M. Taniguchi (RIKEN, Yokohama, Japan) and backcrossed 10 times to C57BL/6J. C57BL/6J wild-type (WT) mice and KO mice bred in a pathogen-free environment. All experiments were performed using male mice. All mice were 12–15 weeks old when they were used for the experiments. The mice were kept under a constant 12 h–12 h light–dark cycle at a temperature of 23–25°C. Standard chow and water were provided.

The transverse aortic constriction (TAC) procedure was performed in WT (WT+TAC; $n = 15$) or KO (KO+TAC; $n = 22$) mice as described by Furihata et al. (2016). Briefly, after being anaesthetized with an I.P. injection of a mixture of 0.3 mg kg⁻¹ of medetomidine (Dorbene; Kyoritsu Seiyaku, Tokyo, Japan), 4.0 mg kg⁻¹ of midazolam (Dormicum; Astellas Pharma, Tokyo, Japan) and 5.0 mg kg⁻¹ of butorphanol (Vetorphale; Meiji Seika Kaisha, Tokyo, Japan), the mouse was intubated and its respiration assisted with a volume-cycled ventilator (Shinano Co., Tokyo, Japan) connected to a 21-gauge cannula inserted into the trachea, with 120 breaths min⁻¹ and a tidal volume of 0.3 ml. A thoracotomy was performed via the second internal costal space at the left upper sternal border. The transverse aortic arch was isolated and ligated between the innominate and left common carotid arteries with an overlying 28-gauge needle, which, after removal of the needle, left a reproducible discrete region of stenosis. After surgery, we administered 5 mg kg⁻¹ s.c. of meloxicam (Metacam; Boehringer Ingelheim, Tokyo, Japan) as an analgesic. A sham operation, without realizing aortic stenosis, was performed in WT (WT+Sham; $n = 7$) and KO (KO+Sham; $n = 7$) mice. During the study period of 2 weeks after surgery, the cages were inspected daily for deceased animals. Mice

that did not eat meals and became immobile early after surgery were euthanized and excluded from the analysis. Euthanasia was performed in four WT+TAC mice and six KO+TAC mice.

Echocardiographic, haemodynamic and organ weight measurements were performed in the surviving mice (WT+Sham, $n = 7$; KO+Sham, $n = 7$; WT+TAC, $n = 10$; and KO+TAC, $n = 10$). For technical reasons, haemodynamic data could not be measured in some mice. After the mice were killed, their hearts were used for histological analysis, immunohistochemical analysis and the quantitative RT-PCR ($n = 4$ – 9 for each group). Given that heart samples from mice are limited in volume, additional mice were used for the flow cytometry analysis ($n = 15$ for each group) and immunoblotting ($n = 3$ – 5 for each group). n represents the number of mice, and data obtained multiple times from the same mice are not included.

2.3 | Isolation of cardiac mononuclear cells

Left ventricular tissue was harvested, minced with fine scissors, placed in 10 ml of RPMI-1640 with 5% fetal bovine serum, 1 mg ml⁻¹ collagenase type IV and 100 U ml⁻¹ DNase I, shaken at 37°C for 45 min, and then triturated through 70 μ m nylon mesh and centrifuged (370 g for 5 min at 4°C). Red blood cells were lysed with Tris-ammonium chloride for 1 min at room temperature. Cardiac mononuclear cells (MNCs) were isolated by density-gradient centrifugation with 12 ml of 33% Percoll as previously described (Homma et al., 2013; Sobirin et al., 2012). Cardiac MNCs from five mice were pooled and subjected to a flow cytometric analysis. All reagents were purchased from Sigma-Aldrich (St Louis, MO, USA). Cardiac cell numbers were determined with Trypan Blue (Wako Pure Chemical Industries, Osaka, Japan).

2.4 | Flow cytometry

To detect iNKT cells, we performed a flow cytometry analysis as previously described (Homma et al., 2013; Sobirin et al., 2012). Cells were incubated with 2.4G2 monoclonal antibody to block the non-specific binding of the primary monoclonal antibody, and then the cells were reacted with α GC-loaded Dimer X (CD1d; Ig recombinant fusion protein), followed by their detection with phycoerythrin-conjugated anti-mouse IgG1 monoclonal antibody. After being washed, the cells were stained with a combination of fluorescein isothiocyanate-anti-T-cell receptor (TCR) β and phycoerythrin-anti-mouse IgG1. These antibodies (except for 2.4G2 monoclonal antibody) were purchased from BD Bioscience Pharmingen (San Diego, CA, USA).

Stained cells were acquired with a FACS Cant II Flow Cytometer (BD Biosciences Immunocytometry Systems, San Jose, CA, USA) and analysed with FlowJo v.7.2.5 software (Flow Jo, Ashland, OR, USA). Propidium iodide (Sigma-Aldrich)-positive cells were electronically gated out from the analysis as dead cells. Each sample population was classified for cell size (forward scatter) and complexity (side scatter), then gated on a population of interest. At least 1.0×10^4 cells were evaluated for each sample. The proportion of Dimer X⁺TCR β ⁺ cells was calculated as the percentage of Dimer X⁺TCR β ⁺ cells among TCR β ⁺ cells.

2.5 | Echocardiographic and haemodynamic measurements

Echocardiographic and haemodynamic measurements of the mice were performed under general anaesthesia with 2–3% isoflurane inhalation. A two-dimensional parasternal short-axis view was obtained at the levels of the papillary muscles. In general, the best views were obtained with the transducer lightly applied to the mid-upper left anterior chest wall. The transducer was then gently moved cephalad or caudad and angulated until desirable images were obtained. After it had been ensured that the imaging was on the axis, two-dimensional targeted M-mode traces were recorded at a paper speed of 50 mm s⁻¹. A 1.4 Fr micromanometer-tipped catheter (Millar Instruments, Houston, TX, USA) was inserted into the right carotid artery and advanced into the LV to measure LV pressures.

2.6 | Tissue preparation and histopathology

After the mice were killed, the heart was excised and dissected into the right ventricle and LV including septum. From the LV tissues, 5- μ m-thick sections were cut and stained with Masson's Trichrome. The myocyte cross-sectional area and collagen volume fraction were determined as previously described (Furihata et al., 2016; Homma et al., 2013; Sobirin et al., 2012).

2.7 | Myocardial matrix metalloproteinase activity

Matrix metalloproteinase (MMP)-2 and MMP-9 activities were determined in LV tissue using a gelatin zymography kit (Primary Cell Co. Ltd, Sapporo, Japan) as we described previously (Sobirin et al., 2012). The zymograms were digitized, and the size-fractionated bands, which indicated proteolytic levels, were measured by the integrated optical density in a rectangular region of interest.

2.8 | Quantitative real-time RT-PCR

Gene expression levels were quantified by real-time RT-PCR as previously described (Homma et al., 2013; Sobirin et al., 2012). Total RNA was extracted from the LV with the use of QuickGene-810 (FujiFilm, Tokyo, Japan) according to the manufacturer's instructions. Complementary DNA (cDNA) was synthesized with a high-capacity cDNA reverse transcription kit (Applied Biosystems, Foster City, CA, USA). A TAqMan quantitative PCR was performed with the 7300 real-time PCR system (Applied Biosystems) to amplify samples for TNF- α , interferon (IFN)- γ , IL-4, IL-10, IL-6, C-C motif chemokine ligand 5 (CCL5), and CCL2 cDNA. These transcripts were normalized to GAPDH. The primers were purchased from Applied Biosystems.

2.9 | Immunoblotting analysis of ERK1/2, JNK, MAPK, STAT3 and human antigen R

Cell lysis and immunoblotting were performed as previously described (Furihata et al., 2016; Homma et al., 2013; Sobirin et al., 2012). Equal amounts of protein extracted from LV tissue were separated

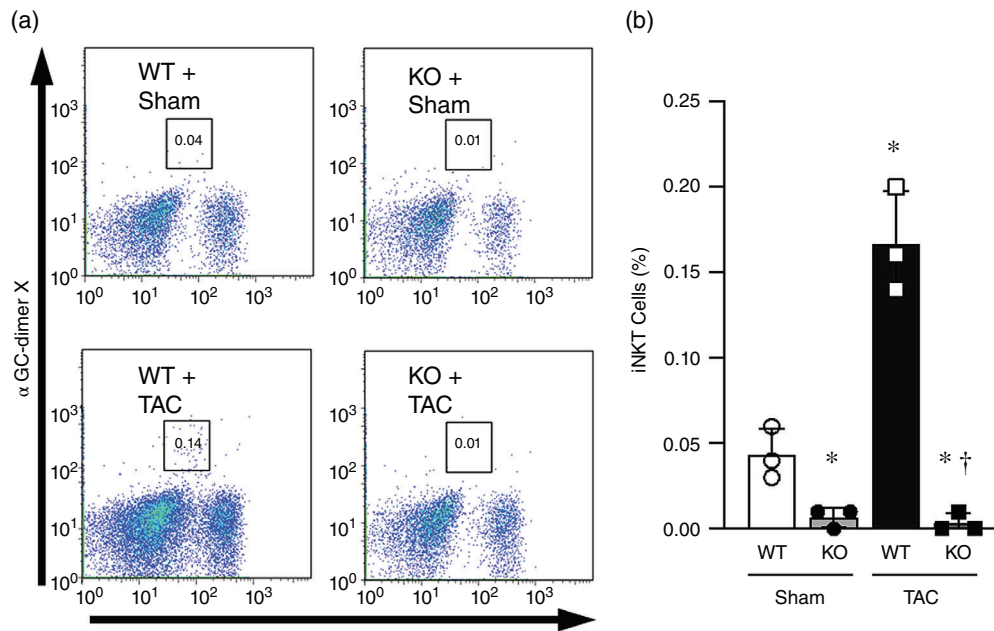


FIGURE 1 Cardiac invariant natural killer T (iNKT) cells were increased after transverse aortic constriction (TAC). (a) Representative flow cytometric assessment of cardiac mononuclear cells obtained from wild-type (WT)+Sham, knockout (KO)+Sham, WT+TAC and KO+TAC mice. Cardiac mononuclear cells from five mice in each group were pooled and analysed. Squares indicate the population of iNKT cells. (b) The ratio of cardiac iNKT cells to mononuclear cells. $n = 3$ for each group. Data are means (SD). * $P < 0.05$ versus WT+Sham. † $P < 0.05$ versus WT+TAC

by SDS-PAGE, transferred to nitrocellulose membranes and blotted with rabbit polyclonal antibodies against phospho-extracellular signal-regulated kinase (p-ERK1/2), phospho-c-Jun N-terminal kinase (p-JNK), phospho-p38 mitogen-activated protein kinase (p-MAPK), phospho-signal transducer and activator of transcription 3 (p-STAT3) and human antigen R (HuR; Millipore, Billerica, MA, USA). Specific bands were labelled with enhanced chemiluminescence and visualized by exposure of the membranes to films. After exposure, the nitrocellulose membranes were blot-stripped using the Re-Blot Plus Western Blot Recycling Kit (Millipore) and re-blotted with rabbit polyclonal antibodies against ERK1/2, JNK, p38 MAPK, STAT3 and rabbit monoclonal antibodies against GAPDH. All antibodies except HuR were purchased from Cell Signaling Technology (Tokyo, Japan).

2.10 | Immunohistochemistry of inflammatory cells

Left ventricular sections were immunostained with antibody against CD3 (Dako, Tokyo, Japan), MAC3 (BD Bioscience Pharmingen) and myeloperoxidase (MPO; Dako), followed by counterstaining with Mayer's Haematoxylin (Homma et al., 2013; Sobirin et al., 2012).

2.11 | Statistical analysis

The data were expressed as the means (SD). A survival analysis was performed by the Kaplan-Meier method, and between-group differences in survival were tested by the log-rank test. The normality of the data was examined using the Shapiro-Wilk test. A between-group comparison of means was performed by two-way ANOVA, followed by Tukey's test. Given that some data were not normally

distributed, their comparisons were tested with the Kruskal-Wallis test, followed by Dunn's comparisons. Values of $P < 0.05$ were considered significant.

3 | RESULTS

3.1 | Invariant natural killer T cells

The flow cytometric analysis revealed that a small number of iNKT cells were present in the LVs from WT+Sham mice. As expected, iNKT cells were not detected in LVs from the KO mice. The proportion of cardiac iNKT cells was increased in the WT+TAC group compared with the WT+Sham group (Figure 1).

3.2 | Survival

No death was observed in the WT+Sham or KO+Sham mice. One WT+TAC mouse and one KO+TAC mouse died for unknown reasons, and five KO+TAC mice died of suspected HF during the 2 weeks after the TAC procedure. The survival rate up to 2 weeks was thus significantly lower in the KO+TAC mice compared with the WT+TAC mice (62.5 versus 90.9%; $P < 0.05$).

3.3 | Echocardiography, haemodynamics and organ weights

The echocardiographic parameters did not differ between the WT+Sham and KO+Sham mice. The LV wall thickness and LV mass/body weight were significantly increased without changes

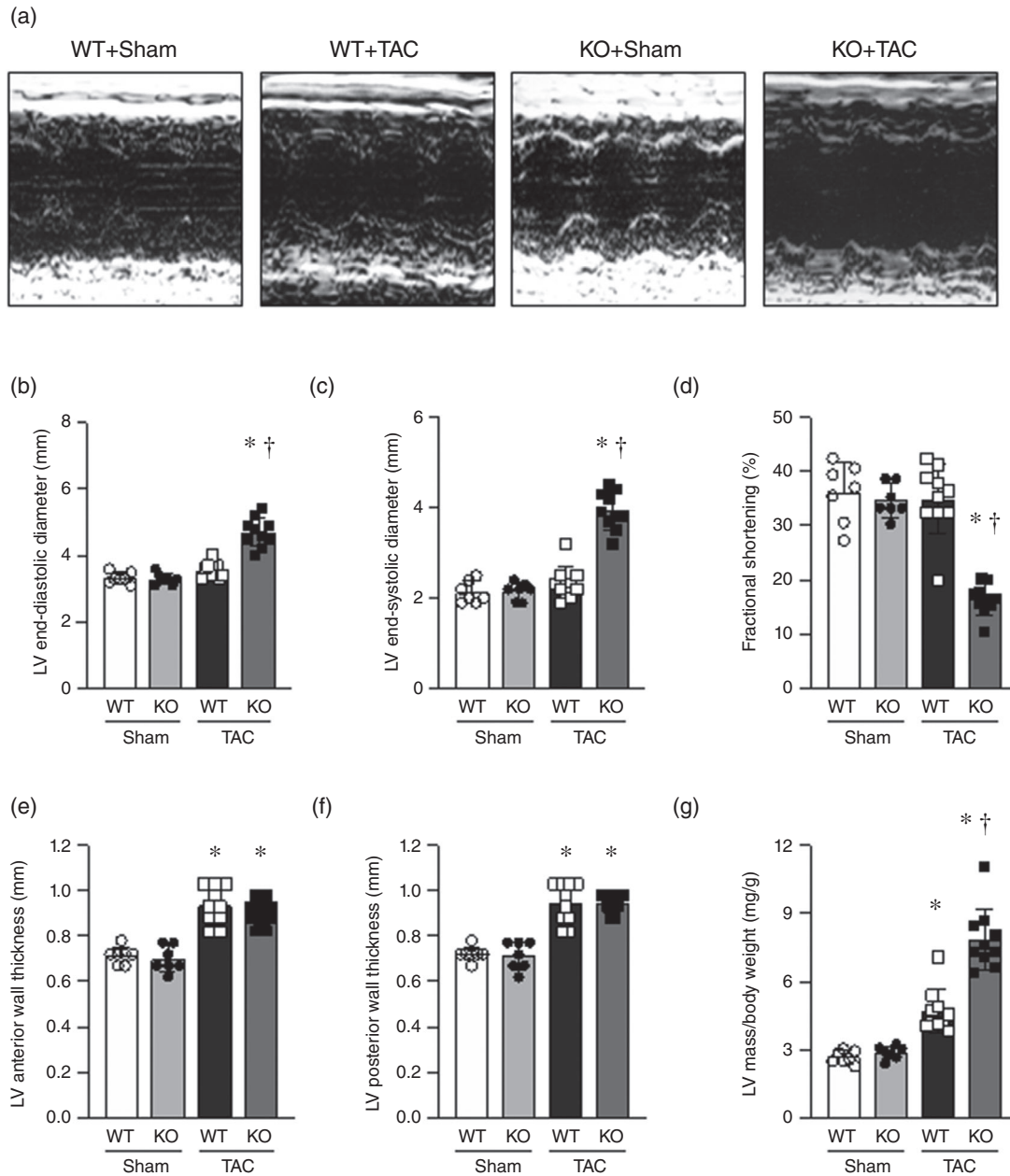


FIGURE 2 The disruption of invariant natural killer T (iNKT) cells exacerbated left ventricular (LV) remodelling. (a) Representative echocardiographic images in wild-type (WT)+Sham, knockout (KO)+Sham, WT+transverse aortic constriction (TAC) and KO+TAC mice. (b–g) Summary data for echocardiographic parameters in WT+Sham ($n = 7$), KO+Sham ($n = 7$), WT+TAC ($n = 10$) and KO+TAC ($n = 10$) mice at 2 weeks after TAC surgery. Data are means (SD). * $P < 0.05$ versus WT+Sham. † $P < 0.05$ versus WT+TAC

in LV diameters or fractional shortening in the WT+TAC mice at 2 weeks after the TAC (Figure 2). The LV diameters were significantly greater and the LV fractional shortening was significantly lower in the KO+TAC mice compared with the WT+TAC mice. The LV wall thickness was comparable between the WT+TAC and KO+TAC groups. However, the LV mass/body weight was significantly increased in the KO+TAC mice compared with the WT+TAC mice.

The haemodynamic data and body and organ weights data are summarized in Table 1. The heart rate and aortic blood pressure were comparable among the four groups of mice. The LV systolic pressure was markedly elevated by the TAC procedure and significantly lower

in the KO+TAC mice compared with the WT+TAC mice. Therefore, the pressure gradient over the TAC was not large in the KO+TAC group compared with the WT+TAC groups at 2 weeks after the TAC surgery. The LV end-diastolic pressure was significantly increased in the WT+TAC mice compared with the WT+Sham mice and tended to be exaggerated in the KO+TAC mice.

The LV dP/dt (positive change in pressure over time) and $-dP/dt$ (negative change in pressure over time) values also tended to be decreased in the KO+TAC group compared with the WT+TAC group, but the difference did not reach statistical significance. There was no significant difference in body weight among the four groups. In

TABLE 1 Haemodynamics, body weight and organ weights at 2 weeks after TAC

| | WT+Sham | KO+Sham | WT+TAC | KO+TAC |
|--|-------------|-------------|---------------|--------------|
| Haemodynamics | | | | |
| <i>n</i> | 4 | 4 | 10 | 7 |
| Heart rate (beats min ⁻¹) | 498 (20) | 474 (31) | 479 (38) | 488 (61) |
| Aortic systolic BP (mmHg) | 95 (2) | 99 (6) | 96 (22) | 93 (13) |
| Aortic diastolic BP (mmHg) | 63 (4) | 71 (8) | 73 (10) | 68 (19) |
| LV systolic pressure (mmHg) | 99 (6) | 101 (4) | 198 (22)* | 164 (24)*† |
| LV end-diastolic pressure (mmHg) | 1.4 (0.6) | 1.8 (1.0) | 5.4 (1.6)* | 7.3 (2.4)* |
| LV +dP/dt (mmHg s ⁻¹) | 8752 (861) | 9992 (1530) | 10,695 (1695) | 7526 (1244) |
| LV -dP/dt (mmHg s ⁻¹) | 7540 (1406) | 6829 (1140) | 8669 (1803) | 6548 (1214) |
| Body and organ weights | | | | |
| <i>n</i> | 7 | 7 | 10 | 10 |
| Body weight (g) | 25.8 (1.7) | 24.8 (2.6) | 26.0 (2.1) | 24.6 (1.3) |
| Heart weight/body weight (mg g ⁻¹) | 4.8 (0.4) | 5.1 (0.5) | 7.2 (1.3)* | 10.0 (0.7)*† |
| LV weight/body weight (mg g ⁻¹) | 3.6 (0.3) | 3.7 (0.4) | 5.6 (1.0)* | 7.6 (0.7)*† |
| Lung weight/body weight (mg g ⁻¹) | 5.5 (0.3) | 5.2 (0.4) | 7.8 (4.5) | 14.6 (4.4)*† |

Data are means (SD).

**P* < 0.05 versus WT+Sham.

†*P* < 0.05 versus WT+TAC.

Abbreviations: BP, blood pressure; +dP/dt, positive change in pressure over time; -dP/dt, negative change in pressure over time; LV, left ventricle; TAC, transverse aortic constriction; and WT, wild-type.

agreement with the echocardiographic LV mass/body weight, the heart weight/body weights and the LV weight/body weights were increased in the WT+TAC group compared with the WT+Sham group and further increased in the KO+TAC group. Moreover, in accordance with the LV end-diastolic pressure, the lung weight/body weight (which is indicative of pulmonary congestion) tended to be increased in the WT+TAC mice and significantly increased in the KO+TAC mice.

3.4 | Histopathology

The Masson's Trichrome staining showed that the myocyte cross-sectional area and the collagen volume fraction were increased in the WT+TAC mice compared with the WT+Sham mice and that these changes were significantly exacerbated in the KO+TAC mice (Figure 3a-c).

3.5 | Myocardial MMP activity

Representative gelatin zymography of the LV tissue from the four groups is shown in Figure 3d. The MMP-2 activity was increased in WT+TAC compared with WT+Sham mice, and this change was significantly increased in KO+TAC mice (Figure 3e). Matrix metalloproteinase-9 activity was not detected in the four groups of mice.

3.6 | Mitogen-activated protein kinase signal

Representative immunoblotting and summary data are shown in Figure 4. The ratio of p-ERK1/2 to total ERK1/2 (p-ERK/ERK) tended to be increased in the WT+TAC group compared with the WT+Sham group. It was significantly increased in the KO+Sham and KO+TAC

groups, and the extent of the increase was greater in the KO+TAC group than in the KO+Sham group. The ratio of p-JNK and p-p38 MAPK to either total did not differ among the four groups of mice.

3.7 | Cytokine gene expressions and cytokine signals

The *IL-10* and *TNF-α* gene expression levels were significantly increased in the WT+TAC mice compared with the WT+Sham mice, and significantly reduced in the KO+TAC mice (Figure 5a, b). Interleukin-6 was increased in the WT+TAC and KO+TAC groups, but did not differ significantly among the groups (Figure 5c). Interferon- γ tended to be increased in the WT+TAC mice, and it was diminished in the KO mice (Figure 5d). Interleukin-4 was not detected in any group.

The ratio of p-STAT3 to total STAT3 (p-STAT3/STAT3) was significantly increased in the TAC mice and was comparable between the WT+TAC and KO+TAC mice (Figure 6). The ratio of HuR/GAPDH was not significantly different among the four groups (Figure 6).

3.8 | Immunohistochemical staining of inflammatory cells and chemokine gene expression

The immunohistochemical stainings for MAC3 and CD3 were barely detectable in the LV tissue from both the WT+Sham and KO+Sham mice. In contrast, they were clearly increased in the WT+TAC and KO+TAC mice (Figure 7a-d). However, there was no significant difference in the infiltration of these cells between the WT+TAC and KO+TAC groups at 2 weeks after TAC. Myeloperoxidase-positive cells were not detected in the LV tissue from all groups of mice. CCL5 was increased in the WT+TAC and KO+TAC group but did not

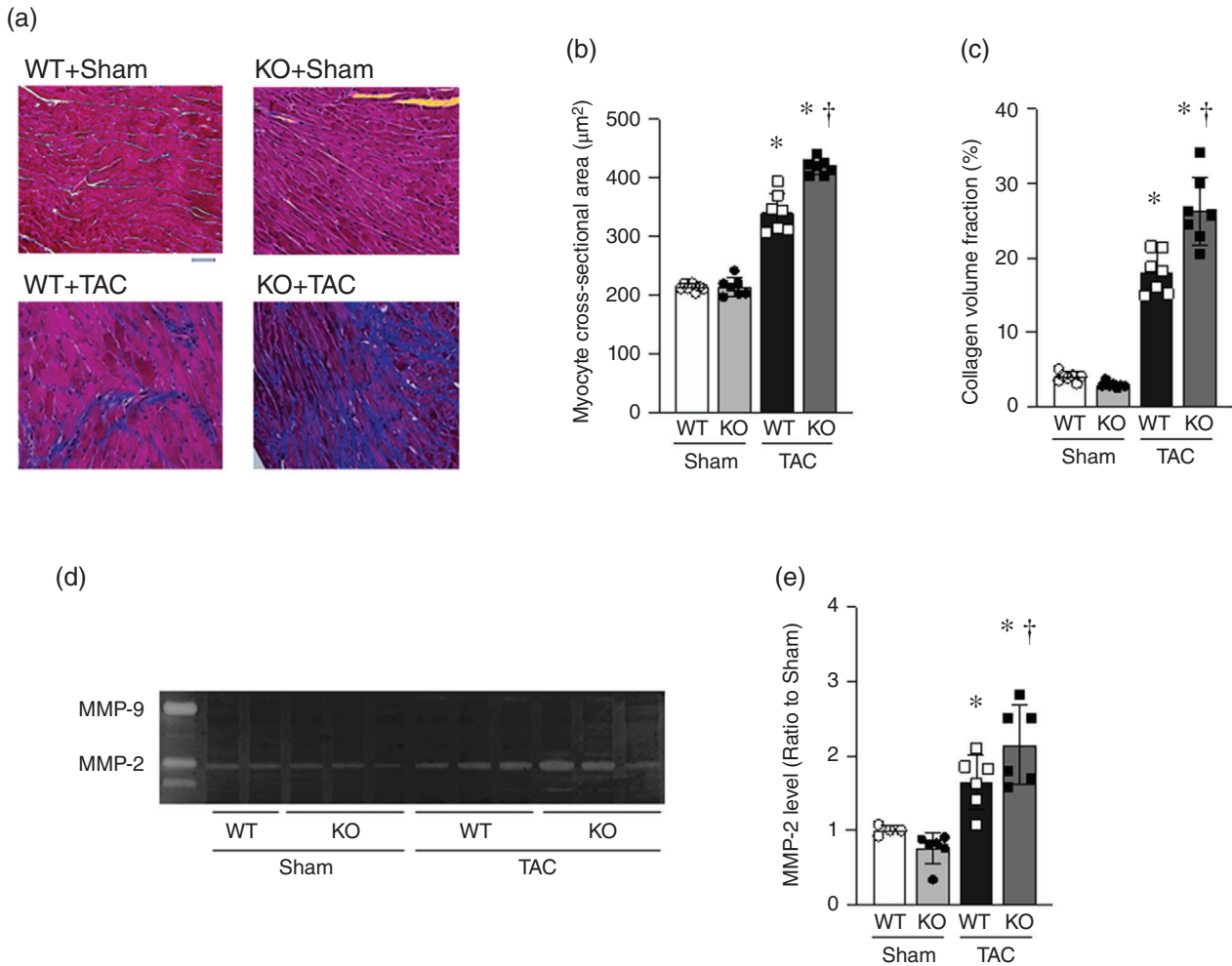


FIGURE 3 The disruption of invariant natural killer T (iNKT) cells exacerbated cardiac hypertrophy and interstitial fibrosis. (a) Representative high-power photomicrographs of left ventricular (LV) cross-sections stained with Masson's Trichrome from wild-type (WT)+Sham, knockout (KO)+Sham, WT+transverse aortic constriction (TAC) and KO+TAC mice. Scale bar: 50 μm . (b, c) Myocyte cross-sectional area (b) and collagen volume fraction (c) were analysed in the four groups of mice ($n = 7$ each). (d, e) Representative LV zymographic matrix metalloproteinase (MMP)-2 and MMP-9 activities in LV (d) and densitometric analysis of MMP-2 (e) ($n = 4-6$ for each). Data are means (SD). * $P < 0.05$ versus WT+Sham. † $P < 0.05$ versus WT+TAC

differ significantly among the groups (Figure 8a). CCL2 tended to be increased in the WT+TAC mice and was diminished in the KO mice (Figure 8b).

4 | DISCUSSION

The most important finding of the present study was that the disruption of iNKT cells exacerbated LV remodelling and hastened the transition to HF after the TAC procedure. Invariant natural killer T cells generally account for a very small proportion of MNCs and have an abundant capacity to produce a mixture of Th1 and Th2 cytokines and a vast array of chemokines. Although there are only a few iNKT cells in the heart and the infiltration of iNKT cells in cardiac hypertrophy increases only a little, the iNKT cells provide the basis for the transition from immunologically chaotic conditions to ordered conditions and orchestrate tissue inflammation. As a result, the infiltration and activation of iNKT cells may compensate for the development of HF.

The echocardiographic data showed that at 2 weeks after surgery, our TAC model exhibited compensated LV hypertrophy with preserved systolic LV function and without overt HF in wild-type mice. In KO mice, the TAC surgery clearly induced decompensated LV hypertrophy, with depressed systolic LV function and overt HF. We could not measure the pressure gradient over the aortic constriction immediately after the TAC surgery in the mice, but it was lower in the KO+TAC mice than in the WT+TAC mice at 2 weeks after the surgery. This suggests that in the KO+TAC mice, the low pressure gradient is attributable to the low LV function. In our preliminary experiment using other sets of WT+TAC and KO+TAC mice, there was no significant difference in the pressure gradient between the two groups immediately after the TAC operation. Therefore, the difference in cardiac phenotype between the WT+TAC and KO+TAC mice could not be explained by the difference in the pressure gradient.

We detected a small number of iNKT cells in LV tissues, and our present findings confirm our previous results (Homma et al., 2013;

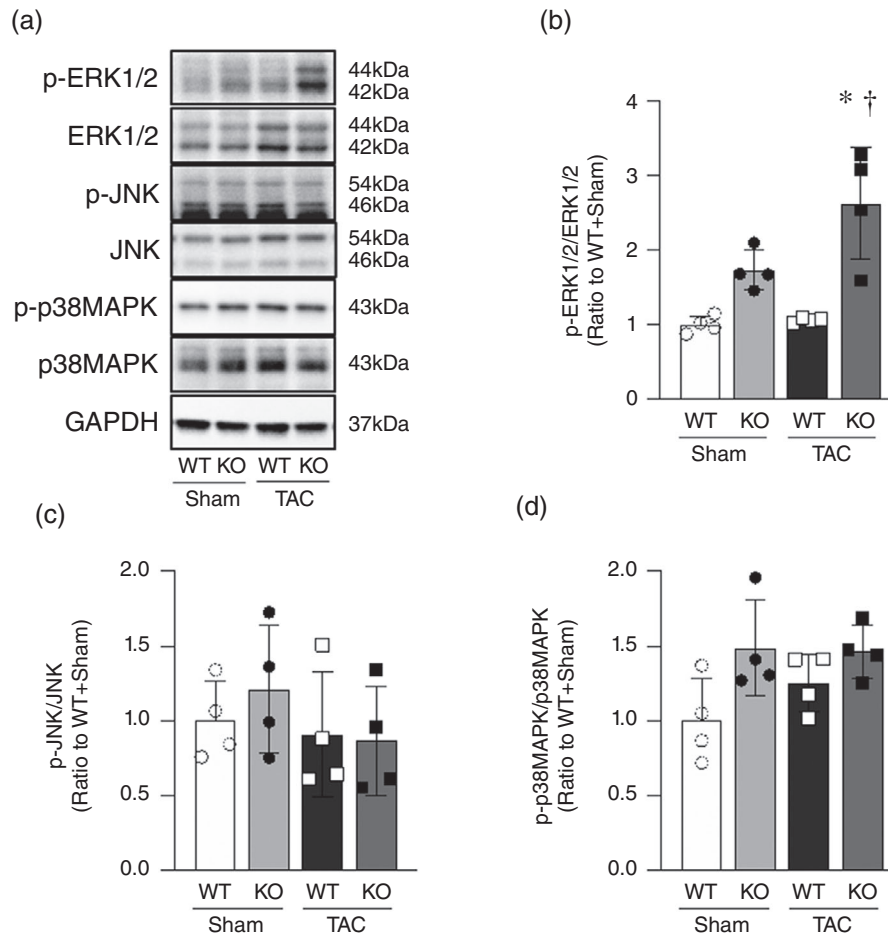


FIGURE 4 The disruption of invariant natural killer T (iNKT) cells increased phosphorylation of extracellular signal-regulated kinase (ERK)1/2. (a–d) Representative immunoblotting analysis and the summary data for p-ERK1/2/ERK1/2, p-JNK/JNK and p-p38MAPK/p38MAPK in left ventricular (LV) tissues from wild-type (WT)+Sham, knockout (KO)+Sham, WT+transverse aortic constriction (TAC) and KO+TAC mice ($n = 4$ each). Data are means (SD). * $P < 0.05$ versus WT+Sham. † $P < 0.05$ versus WT+TAC

Sobirin et al., 2012). Here, in a preliminary experiment conducted to validate the detection of iNKT cells by the flow cytometry analysis, we evaluated spleen MNCs. Invariant natural killer T cells were clearly detected in the spleens from WT mice but not KO mice. Generally, the proportion of MNCs that are iNKT cells is ~10–20% in mouse liver, 1.5% in mouse spleen, 0.5% in mouse thymus and 0.01–0.5% in human peripheral blood (Lee, Benlagha, Teyton, & Bendelac, 2002a; Lee et al., 2002b; Watarai, Nakagawa, Omori-Miyake, Dashtsoodol, & Taniguchi, 2008). It is thus not surprising that a very small proportion of iNKT cells among MNCs was detected in the mouse hearts. The important point is that the iNKT cells were increased approximately threefold in WT+TAC mice. The significance of this increase was revealed using KO mice in the present study.

The protective role of iNKT cells has been shown to include major two mechanisms: a shift from Th1 towards a Th2 pattern, and the induction of the immunosuppressive cytokine IL-10 in Th1-like autoimmune diseases (Croxford, Miyake, Huang, Shimamura, & Yamamura, 2006). Our present findings also showed that IL-10 was increased in the LV from WT+TAC mice and decreased in the LV from KO+TAC mice in association with the changes in iNKT cells.

Interleukin-10 can inhibit the production of pro-inflammatory cytokines by macrophages and Th1 cells and directly promote the death of inflammatory cells (Fiorentino, Zlotnik, Mosmann, Howard, & O'Garra, 1991a; Fiorentino et al., 1991b; Forster, Vieira, & Rajewsky, 1989). Beyond its suppressive effects on inflammatory gene synthesis, IL-10 could also regulate the extracellular matrix and angiogenesis (Apte, Richter, Herndon, & Ferguson, 2006; Dace, Khan, Kelly, & Apte, 2008; Lacraz, Nicod, Chicheportiche, Welgus, & Dayer, 1995; Silvestre et al., 2000). Krishnamurthy et al. (2009) showed that IL-10 suppressed inflammation and attenuated LV remodelling after MI in mice by inhibiting fibrosis via the suppression of HuR and the activation of STAT3. However, we did not observe any significant differences in STAT3 activation or HuR expression between the WT+TAC and KO+TAC mice.

The present study also showed that TNF- α was increased in LV from WT+TAC mice and decreased in LV from KO+TAC mice. Tumour necrosis factor- α is a pro-inflammatory cytokine that is considered to be cardiotoxic and to induce LV dysfunction (Kubota et al., 1997; Sun et al., 2007). However, TNF- α also has protective effects during the maladaptive transition to HF (Higuchi et al., 2004; Hirota et al., 1999).

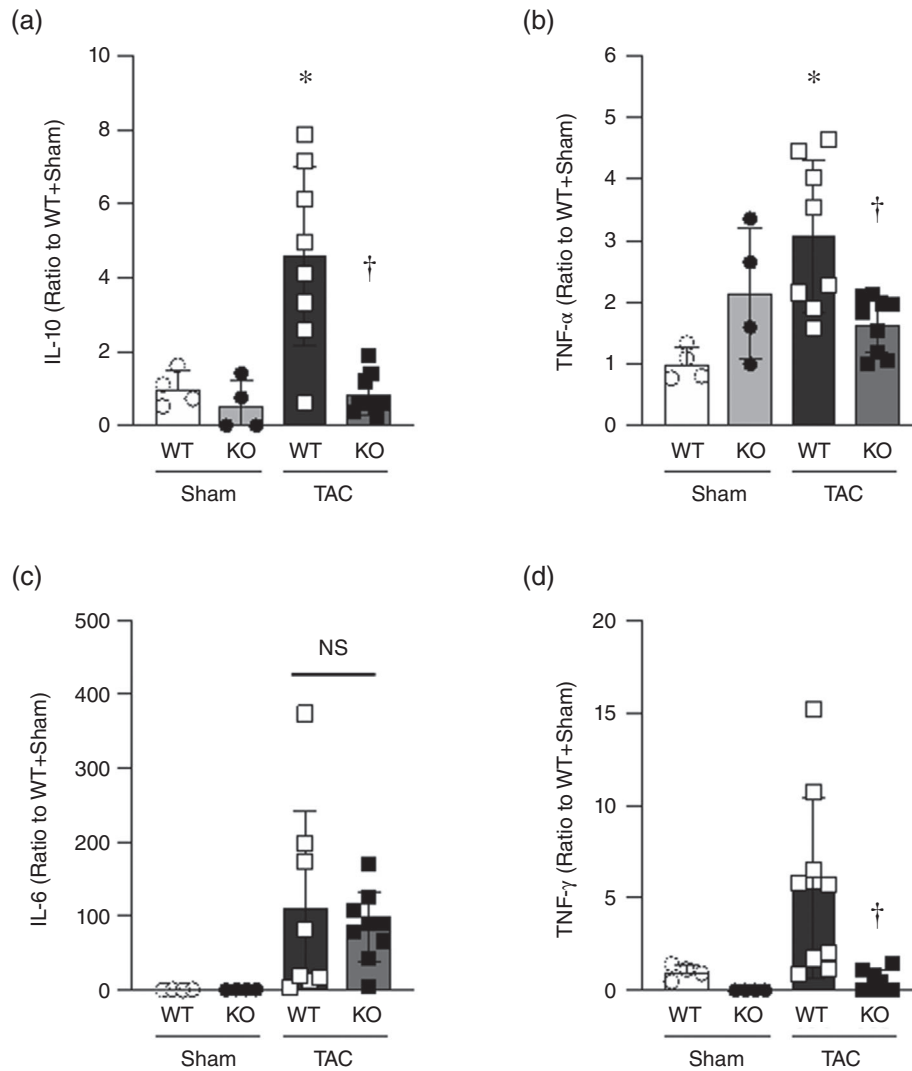


FIGURE 5 The disruption of invariant natural killer T (iNKT) cells altered mRNA expressions of cytokines. (a–d) Quantitative analysis of the mRNA expressions of *IL-10*, *TNF- α* , *IL-6* and *IFN- γ* in the left ventricle (LV) from the four groups of mice ($n = 4$ – 9 for each). The mRNA expressions were normalized to *GAPDH* expression and are depicted as the ratio to wild-type (WT)+Sham. Data are means (SD). * $P < 0.05$ versus WT+Sham. † $P < 0.05$ versus WT+transverse aortic constriction (TAC)

The treatment of patients with HF with either soluble TNF receptor (the RENEWAL study) or an anti-TNF antibody (the ATTACH trial) did not show clinical benefits (Chung, Packer, Lo, Fasanmade, & Willerson, 2003; Mann et al., 2004). A decrease in the ratio of IL-10 to TNF- α was reported to be correlated with depressed cardiac function (Kaur, Sharma, & Singal, 2006). These findings are consistent with our present observation that the ratio of mRNA expression of *IL-10* to *TNF- α* was significantly less in the KO+TAC group compared with the WT+TAC group (0.54 ± 0.14 versus 1.47 ± 0.23 , $P < 0.05$). These findings suggest that investigations of the underlying mechanisms of inflammation in the development of HF should focus on the modulation of the cytokine balance rather than on individual cytokines. Given that iNKT cells can function as a bridge between the innate and adaptive immune systems, they might act as an upstream regulator of the cytokine balance in the pressure-overloaded heart.

Matrix metalloproteinase-2 is ubiquitously distributed in cardiac myocytes and fibroblasts and plays a crucial role in the development of cardiac remodelling in response to pressure overload (Cheung, Sawicki, Wozniak, Radomski, & Schulz, 2000; Matsusaka et al., 2006). Our previous data showed that the selective disruption of the *MMP-2* gene attenuated interstitial fibrosis in LV hypertrophy after TAC (Matsusaka et al., 2006). Therefore, it has been suggested that the activation of MMP-2 might play an important role in development of interstitial fibrosis in our model. However, the mechanisms responsible for the activation of MMP-2 by the deletion of iNKT cells remain to be determined.

The MAPK signalling pathways consist of a sequence of successively functioning kinases that ultimately result in the dual phosphorylation and activation of p38, JNKs and ERKs (Garrington & Johnson, 1999). Notably, the activation of the MEK1-ERK1/2 pathway has

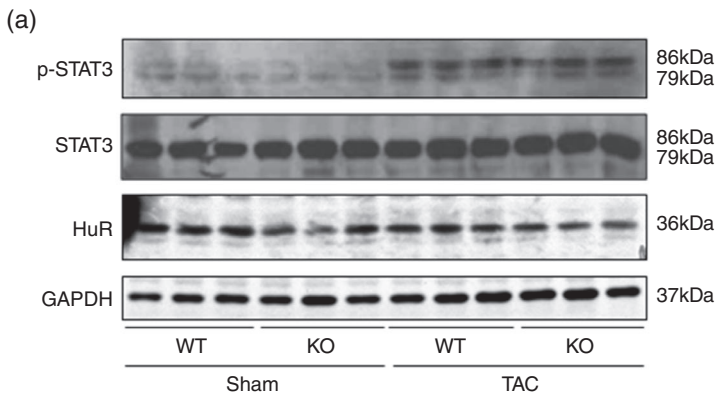
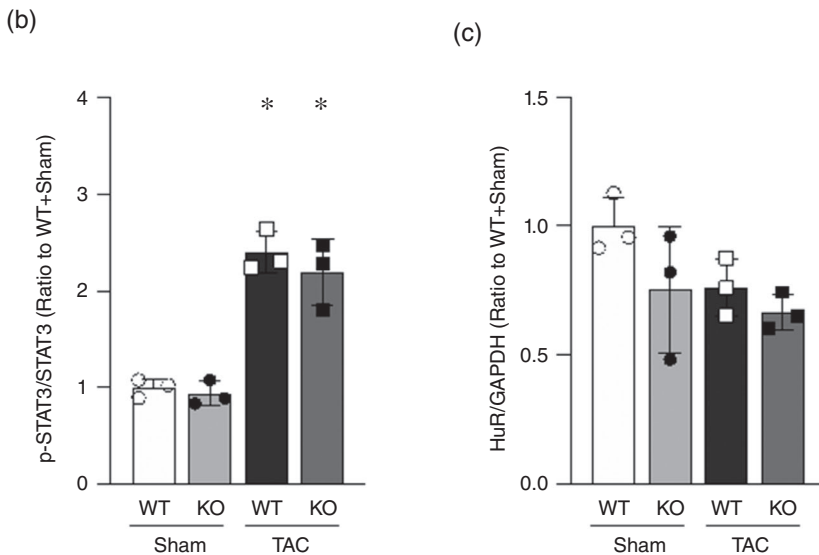


FIGURE 6 The disruption of invariant natural killer T (iNKT) cells did not affect cytokine signals. (a–c) Representative immunoblotting analysis and the summary data for p-STAT3/STAT3 and HuR/GAPDH in left ventricular (LV) tissues from the four groups of mice ($n = 3$ each). Data are means (SD). * $P < 0.05$ versus wild-type (WT)+Sham



been shown to induce cardiac hypertrophy, and the reduction of MEK–ERK1/2 activity inhibits interstitial fibrosis and cardiac dysfunction *in vivo* (Buono et al., 2000; Thum et al., 2008). We demonstrated that the phosphorylation of ERKs was significantly increased in KO mice compared with WT mice, and it was markedly enhanced in KO+TAC mice. These data thus indicate that ERK signalling might be one of the regulatory factors in the exacerbation of myocyte hypertrophy and interstitial fibrosis after TAC in KO mice. MAPKs are regulated by reversible phosphorylation, and this is attributable to phosphatase-mediated dephosphorylation by MAPK phosphatases (MKP; Keyse, 2000). The overexpression of MKP-1 can inhibit cardiac hypertrophy via the dephosphorylation of ERK, and the downregulation of MKP-1 can lead to cardiac hypertrophy via the phosphorylation of ERK (Hayashi et al., 2004). Immunological factors have been noted to alter MKP-1 expression (Wancket, Frazier, & Liu, 2012). Pro-inflammatory cytokines reduce the expression of MKP-1, and anti-inflammatory cytokines increase the expression of MKP-1. Therefore, the enhanced phosphorylation of ERK in KO+TAC mice might be attributable to downregulation of MKP-1 by disordered immunological conditions.

There are several limitations to be acknowledged in the present study. First, we could not demonstrate a conclusive role of iNKT cells

in the development of cardiac remodelling after TAC, although we performed the experiments using iNKT cell KO mice. The best method to clarify this issue would be a rescue experiment using adoptive transfer of iNKT cells to KO mice. Unfortunately, we could not complete this experiment owing to technical difficulties. Second, we could not demonstrate clear evidence for the role of other immune cells in the exacerbation of cardiac remodelling in iNKT KO mice. Weisheit et al. (2014) reported that macrophages and neutrophils were increased in the heart at 3–6 days after TAC. At 21 days after TAC, these tended to be increased, but were not significantly different. In particular, an accumulation of Ly6C^{low} macrophages, tissue-repairing macrophages, was dominant. Nevers et al. (2015) reported that T cells were increased in the heart at 2–4 weeks, but not 48 h after TAC. They also showed that neutrophils and macrophages in the heart did not differ at 48 h, 2 and 4 weeks after TAC. They clarified, using T-cell-deficient mice, that the infiltration of T cells in the heart played a crucial role in the development of cardiac remodelling after TAC. Invariant natural killer T cell-derived cytokines can activate many immune cells, including T cells, macrophages and neutrophils (Kronenberg et al., 2002). Therefore, the changes in cardiac phenotype we observed in iNKT cell KO mice might be associated with the changes in macrophages and T cells at a time point earlier than 2 weeks. Further investigations are

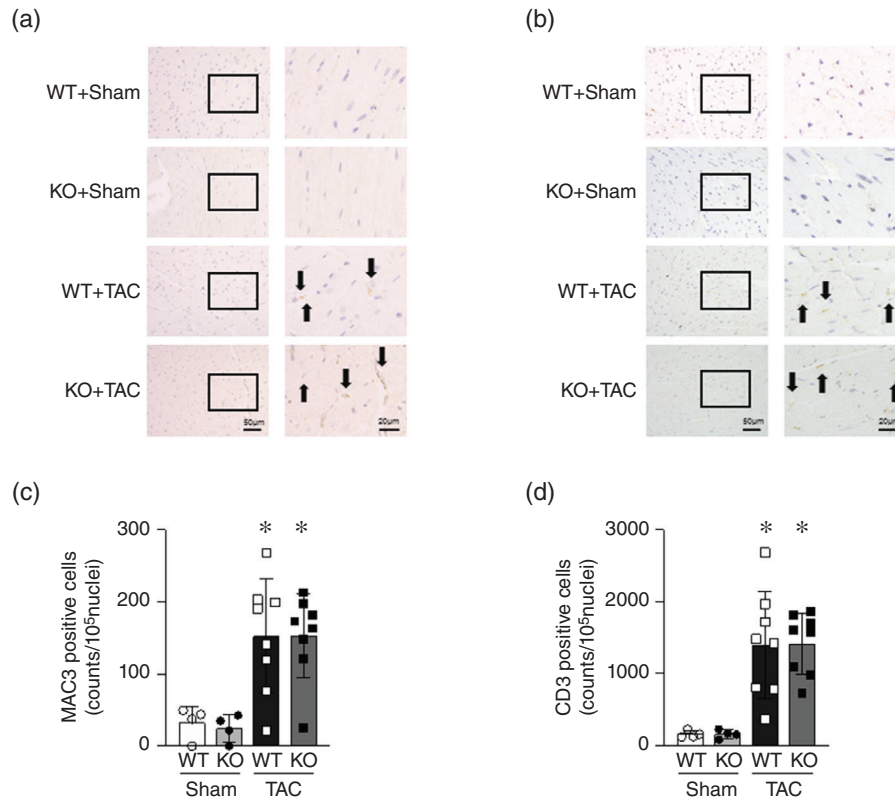


FIGURE 7 The disruption of invariant natural killer T (iNKT) cells did not affect the infiltration of MAC3⁺ and CD3⁺ cells at 2 weeks. (a, b) Representative photomicrographs of left ventricular (LV) cross-sections stained with anti-MAC3 and anti-CD3 in wild-type (WT)+Sham, knockout (KO)+Sham, WT+ transverse aortic constriction (TAC) and KO+TAC mice. Each right-hand panel shows a magnified image of the square portion in each left-hand panel. Black arrows indicate cells staining positive. (c, d) Summary data of the numbers of MAC3⁺ and CD3⁺ cells in the LV ($n = 4-8$ for each). Data are means (SD). * $P < 0.05$ versus WT+Sham

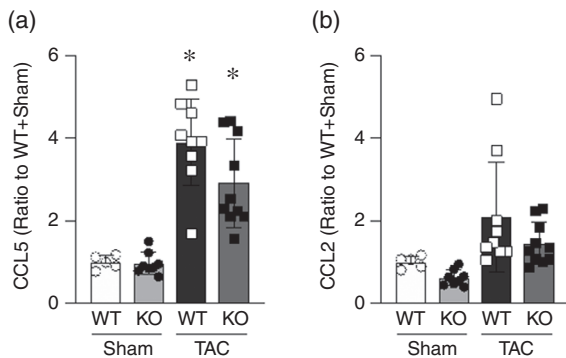


FIGURE 8 The disruption of invariant natural killer T (iNKT) cells did not affect the mRNA expressions of C-C motif chemokine ligand 5 (CCL5) and CCL2. (a, b) Quantitative analysis of the mRNA expressions of CCL5 and CCL2 in the left ventricle (LV) from the four groups of mice ($n = 5-10$ each). The mRNA expressions were normalized to the GAPDH expression and are depicted as the ratio to wild-type (WT)+Sham. Data are means (SD). * $P < 0.05$ versus WT+Sham

required to elucidate the role of other immune cells. Finally, protein levels of several cytokines, including TNF- α and IL-10, could not be detected in the heart by immunohistochemical staining and flow cytometry analysis, as in our previous studies (Homma et al., 2013; Sobirin et al., 2012). This might be attributable to their short half-lives and the small amount of cytokine protein in the heart.

In summary, the results of the present study demonstrated, for the first time, that the disruption of iNKT cells exacerbated the development of cardiac remodelling and HF after TAC. This suggests that iNKT cells play a protective role against HF caused by pressure overload. Our findings provide new mechanistic insights and might provide a basis for a new therapeutic target for HF.

ACKNOWLEDGEMENTS

We thank Ms Kaoruko Kawai for her technical assistance and Drs Masaru Taniguchi and Toshinori Nakayama for their professional advice.

COMPETING INTERESTS

None declared.

AUTHOR CONTRIBUTIONS

All experiments were conducted at the Department of Cardiovascular Medicine, Faculty of Medicine and Graduate School of Medicine, Hokkaido University. S.K. and H.T. conceived and designed the research. M.T., S.T., N.K., T.F., A.F., Y.O. and A.S. performed the experiments. M.T., S.T. and M.A.S. analysed the data. S.K., N.I. and K.I.

interpreted the results of the experiments. M.T., S.K. and S.T. drafted the manuscript. N.K., T.F., M.A.S., A.F., Y.O., N.I., K.I. and H.T. edited and revised the manuscript. All authors approved the final version of the manuscript and agree to be accountable for all aspects of the work in ensuring that questions related to the accuracy or integrity of any part of the work are appropriately investigated and resolved. All persons designated as authors qualify for authorship, and all those who qualify for authorship are listed.

ORCID

Shintaro Kinugawa  <https://orcid.org/0000-0003-2559-0054>

Shingo Takada  <https://orcid.org/0000-0002-7781-9482>

REFERENCES

- Apte, R. S., Richter, J., Herndon, J., & Ferguson, T. A. (2006). Macrophages inhibit neovascularization in a murine model of age-related macular degeneration. *PLoS Medicine*, 3, e310.
- Bueno, O. F., De Windt, L. J., Tymitz, K. M., Witt, S. A., Kimball, T. R., Klevitsky, R., ... Molkentin, J. D. (2000). The MEK1-ERK1/2 signaling pathway promotes compensated cardiac hypertrophy in transgenic mice. *The EMBO Journal*, 19, 6341-6350.
- Cheung, P. Y., Sawicki, G., Wozniak, M., Radomski, M. W., & Schulz, R. (2000). Matrix metalloproteinase-2 contributes to ischemia-reperfusion injury in the heart. *Circulation*, 101, 1833-1839.
- Chung, E. S., Packer, M., Lo, K. H., Fasanmade, A. A., & Willerson, J. T.; Anti-TNF Therapy Against Congestive Heart Failure Investigators. (2003) Randomized, double-blind, placebo-controlled, pilot trial of infliximab, a chimeric monoclonal antibody to tumor necrosis factor- α , in patients with moderate-to-severe heart failure: Results of the anti-TNF Therapy Against Congestive Heart Failure (ATTACH) trial. *Circulation*, 107, 3133-3140.
- Croxford, J. L., Miyake, S., Huang, Y. Y., Shimamura, M., & Yamamura, T. (2006). Invariant V α 19i T cells regulate autoimmune inflammation. *Nature Immunology*, 7, 987-994.
- Cui, J., Shin, T., Kawano, T., Sato, H., Kondo, E., Taura, I., ... Taniguchi, M. (1997). Requirement for V α 14 NKT cells in IL-12-mediated rejection of tumors. *Science*, 278, 1623-1626.
- Dace, D. S., Khan, A. A., Kelly, J., & Apte, R. S. (2008). Interleukin-10 promotes pathological angiogenesis by regulating macrophage response to hypoxia during development. *PLoS ONE*, 3, e3381.
- Fiorentino, D. F., Zlotnik, A., Mosmann, T. R., Howard, M., & O'Garra, A. (1991a). IL-10 inhibits cytokine production by activated macrophages. *Journal of Immunology*, 147, 3815-3822.
- Fiorentino, D. F., Zlotnik, A., Vieira, P., Mosmann, T. R., Howard, M., Moore, K. W., & O'Garra, A. (1991b). IL-10 acts on the antigen-presenting cell to inhibit cytokine production by Th1 cells. *Journal of Immunology*, 146, 3444-3451.
- Fischer, P., & Hilfiker-Kleiner, D. (2007). Survival pathways in hypertrophy and heart failure: The gp130-STAT axis. *Basic Research in Cardiology*, 102, 393-411.
- Forster, I., Vieira, P., & Rajewsky, K. (1989). Flow cytometric analysis of cell proliferation dynamics in the B cell compartment of the mouse. *International Immunology*, 1, 321-331.
- Furihata, T., Kinugawa, S., Takada, S., Fukushima, A., Takahashi, M., Homma, T., ... Tsutsui, H. (2016). The experimental model of transition from compensated cardiac hypertrophy to failure created by transverse aortic constriction in mice. *International Journal of Cardiology. Heart & Vasculature*, 11, 24-28.
- Garrington, T. P., & Johnson, G. L. (1999). Organization and regulation of mitogen-activated protein kinase signaling pathways. *Current Opinion in Cell Biology*, 11, 211-218.
- Godfrey, D. I., MacDonald, H. R., Kronenberg, M., Smyth, M. J., & Van Kaer, L. (2004). NKT cells: What's in a name? *Nature Reviews Immunology*, 4, 231-237.
- Hayashi, D., Kudoh, S., Shiojima, I., Zou, Y., Harada, K., Shimoyama, M., ... Komuro, I. (2004). Atrial natriuretic peptide inhibits cardiomyocyte hypertrophy through mitogen-activated protein kinase phosphatase-1. *Biochemical and Biophysical Research Communications*, 322, 310-319.
- Higuchi, Y., McTiernan, C. F., Frye, C. B., McGowan, B. S., Chan, T. O., & Feldman, A. M. (2004). Tumor necrosis factor receptors 1 and 2 differentially regulate survival, cardiac dysfunction, and remodeling in transgenic mice with tumor necrosis factor- α -induced cardiomyopathy. *Circulation*, 109, 1892-1897.
- Hirota, H., Chen, J., Betz, U. A., Rajewsky, K., Gu, Y., Ross, J., ... Chien, K. R. (1999). Loss of a gp130 cardiac muscle cell survival pathway is a critical event in the onset of heart failure during biomechanical stress. *Cell*, 97, 189-198.
- Homma, T., Kinugawa, S., Takahashi, M., Sobirin, M. A., Saito, A., Fukushima, A., ... Tsutsui, H. (2013). Activation of invariant natural killer T cells by α -galactosylceramide ameliorates myocardial ischemia/reperfusion injury in mice. *Journal of Molecular and Cellular Cardiology*, 62, 179-188.
- Hong, S., Wilson, M. T., Serizawa, I., Wu, L., Singh, N., Naidenko, O. V., ... Van Kaer, L. (2001). The natural killer T-cell ligand α -galactosylceramide prevents autoimmune diabetes in non-obese diabetic mice. *Nature Medicine*, 7, 1052-1056.
- Kaur, K., Sharma, A. K., & Singal, P. K. (2006). Significance of changes in TNF- α and IL-10 levels in the progression of heart failure subsequent to myocardial infarction. *American Journal of Physiology-Heart and Circulatory Physiology*, 291, H106-H113.
- Kawano, T., Cui, J., Koezuka, Y., Taura, I., Kaneko, Y., Motoki, K., ... Taniguchi, M. (1997). CD1d-restricted and TCR-mediated activation of V α 14 NKT cells by glycosylceramides. *Science*, 278, 1626-1629.
- Keyse, S. M. (2000). Protein phosphatases and the regulation of mitogen-activated protein kinase signalling. *Current Opinion in Cell Biology*, 12, 186-192.
- Krishnamurthy, P., Rajasingh, J., Lambers, E., Qin, G., Losordo, D. W., & Kishore, R. (2009). IL-10 inhibits inflammation and attenuates left ventricular remodeling after myocardial infarction via activation of STAT3 and suppression of HuR. *Circulation Research*, 104, e9-e18.
- Kronenberg, M., & Gapin, L. (2002). The unconventional lifestyle of NKT cells. *Nature Reviews Immunology*, 2, 557-568.
- Kubota, T., McTiernan, C. F., Frye, C. S., Slawson, S. E., Lemster, B. H., Koretsky, A. P., ... Feldman, A. M. (1997). Dilated cardiomyopathy in transgenic mice with cardiac-specific overexpression of tumor necrosis factor- α . *Circulation Research*, 81, 627-635.
- Lacraz, S., Nicod, L. P., Chicheportiche, R., Welgus, H. G., & Dayer, J. M. (1995). IL-10 inhibits metalloproteinase and stimulates TIMP-1 production in human mononuclear phagocytes. *The Journal of Clinical Investigation*, 96, 2304-2310.
- Lee, P. T., Benlagha, K., Teyton, L., & Bendelac, A. (2002a). Distinct functional lineages of human V α 24 natural killer T cells. *The Journal of Experimental Medicine*, 195, 637-641.
- Lee, P. T., Putnam, A., Benlagha, K., Teyton, L., Gottlieb, P. A., & Bendelac, A. (2002b). Testing the NKT cell hypothesis of human IDDM pathogenesis. *The Journal of Clinical Investigation*, 110, 793-800.
- Mann, D. L., McMurray, J. J., Packer, M., Swedberg, K., Borer, J. S., Colucci, W. S., ... Fleming, T. (2004). Targeted anticytokine therapy in patients with chronic heart failure: Results of the Randomized Etanercept Worldwide Evaluation (RENEWAL). *Circulation*, 109, 1594-1602.
- Matsuda, J. L., Mallewaey, T., Scott-Browne, J., & Gapin, L. (2008). CD1d-restricted iNKT cells, the 'Swiss-Army knife' of the immune system. *Current Opinion in Immunology*, 20, 358-368.

- Matsusaka, H., Ide, T., Matsushima, S., Ikeuchi, M., Kubota, T., Sunagawa, K., ... Tsutsui, H. (2006). Targeted deletion of matrix metalloproteinase 2 ameliorates myocardial remodeling in mice with chronic pressure overload. *Hypertension*, *47*, 711–717.
- Miellot, A., Zhu, R., Diem, S., Boissier, M. C., Herbelin, A., & Bessis, N. (2005). Activation of invariant NK T cells protects against experimental rheumatoid arthritis by an IL-10-dependent pathway. *European Journal of Immunology*, *35*, 3704–3713.
- Nevers, T., Salvador, A. M., Grodecki-Pena, A., Knapp, A., Velázquez, F., Aronovitz, M., ... Alcaide, P. (2015). Left ventricular T-cell recruitment contributes to the pathogenesis of heart failure. *Circulation: Heart Failure*, *8*, 776–787.
- Nicoletti, A., & Michel, J. B. (1999). Cardiac fibrosis and inflammation: Interaction with hemodynamic and hormonal factors. *Cardiovascular Research*, *41*, 532–543.
- Rogers, L., Burchat, S., Gage, J., Hasu, M., Thabet, M., Willcox, L., ... Whitman, S. C. (2008). Deficiency of invariant V α 14 natural killer T cells decreases atherosclerosis in LDL receptor null mice. *Cardiovascular Research*, *78*, 167–174.
- Sharif, S., Arreaza, G. A., Zucker, P., Mi, Q. S., Sondhi, J., Naidenko, O. V., ... Herbelin, A. (2001). Activation of natural killer T cells by α -galactosylceramide treatment prevents the onset and recurrence of autoimmune Type 1 diabetes. *Nature Medicine*, *7*, 1057–1062.
- Silvestre, J. S., Mallat, Z., Duriez, M., Tamarat, R., Bureau, M. F., Scherman, D., ... Levy, B. I. (2000). Antiangiogenic effect of interleukin-10 in ischemia-induced angiogenesis in mice hindlimb. *Circulation Research*, *87*, 448–452.
- Singh, A. K., Wilson, M. T., Hong, S., Olivares-Villagómez, D., Du, C., Stanic, A. K., ... Van Kaer, L. (2001). Natural killer T cell activation protects mice against experimental autoimmune encephalomyelitis. *The Journal of Experimental Medicine*, *194*, 1801–1811.
- Sobirin, M. A., Kinugawa, S., Takahashi, M., Fukushima, A., Homma, T., Ono, T., ... Tsutsui, H. (2012). Activation of natural killer T cells ameliorates postinfarct cardiac remodeling and failure in mice. *Circulation Research*, *111*, 1037–1047.
- Sun, M., Chen, M., Dawood, F., Zurawska, U., Li, J. Y., Parker, T., ... Liu, P. (2007). Tumor necrosis factor- α mediates cardiac remodeling and ventricular dysfunction after pressure overload state. *Circulation*, *115*, 1398–1407.
- Takada, S., Masaki, Y., Kinugawa, S., Matsumoto, J., Furihata, T., Mizushima, W., ... Tsutsui, H. (2016). Dipeptidyl peptidase-4 inhibitor improved exercise capacity and mitochondrial biogenesis in mice with heart failure via activation of glucagon-like peptide-1 receptor signalling. *Cardiovascular Research*, *111*, 338–347.
- Thum, T., Gross, C., Fiedler, J., Fischer, T., Kissler, S., Bussen, M., ... Engelhardt, S. (2008). MicroRNA-21 contributes to myocardial disease by stimulating MAP kinase signalling in fibroblasts. *Nature*, *456*, 980–984.
- Wancket, L. M., Frazier, W. J., & Liu, Y. (2012). Mitogen-activated protein kinase phosphatase (MKP)-1 in immunology, physiology, and disease. *Life Sciences*, *90*, 237–248.
- Watarai, H., Nakagawa, R., Omori-Miyake, M., Dashtsoodol, N., & Taniguchi, M. (2008). Methods for detection, isolation and culture of mouse and human invariant NKT cells. *Nature Protocols*, *3*, 70–78.
- Weisheit, C., Zhang, Y., Faron, A., Köpke, O., Weisheit, G., Steinsträsser, A., ... Baumgarten, G. (2014). Ly6C^{low} and not Ly6C^{high} macrophages accumulate first in the heart in a model of murine pressure-overload. *PLoS ONE*, *9*, e112710.
- Xia, Y., Lee, K., Li, N., Corbett, D., Mendoza, L., & Frangogiannis, N. G. (2009). Characterization of the inflammatory and fibrotic response in a mouse model of cardiac pressure overload. *Histochemistry and Cell Biology*, *131*, 471–481.

How to cite this article: Takahashi M, Kinugawa S, Takada S, et al. The disruption of invariant natural killer T cells exacerbates cardiac hypertrophy and failure caused by pressure overload in mice. *Experimental Physiology*. 2020;1–13. <https://doi.org/10.1113/EP087652>